



# Quasi-static uniaxial cyclic loading protocol for RC columns representing wall boundary zones

*R.A. Gokhale, R.P. Dhakal, M. Tripathi & F. Dashti*

University of Canterbury, Christchurch.

## ABSTRACT

Seismic performance of a flexurally-dominated reinforced concrete wall is dependent on the response of its end boundary zones. In order to evaluate the performance of structural walls, a common practice adopted in laboratories is to test reinforced concrete columns representing the corresponding wall boundaries under uniaxial cyclic loading. This paper presents a numerical investigation leading to development of a quasi-static uniaxial cyclic loading protocol based on the inelastic strain demands at the wall boundaries, when the corresponding structural wall is subjected to earthquake ground motions of various characteristics. With the increasing emphasis on the performance-based design, the proposed loading protocol is structured around the inelastic strain demands generated at the performance-based drift limits of structural walls. Non-linear time history analyses are carried out on a numerical wall model to obtain the average strain histories at the wall boundaries. A statistical evaluation of the number of inelastic cycles and the corresponding strain ranges form the main basis for the load history development. As the damage is predominantly caused due to repeated large inelastic strain excursions, rain flow counting method has been utilized for counting and sorting of the inelastic cycles. The proposed cyclic uniaxial strain histories are more representative of the cumulative demands imposed by moderate-to-large magnitude earthquakes, and their application would facilitate a more rational assessment of the seismic performance of flexurally-dominated RC walls than the current approach of testing boundary zones under arbitrarily decided tension-compression cycles.

## 1 INTRODUCTION

Reinforced concrete (RC) structural walls provide relatively high in-plane stiffness and are therefore considered as the preferred lateral load resisting system in regions of medium to high seismicity.

Performance of a flexurally-dominated RC wall against in-plane lateral cyclic actions depends on the response of its confined end regions known as the boundary zones. These end regions (or boundary zones) are subjected to tensile and compressive strain reversals during seismic events. Seismic design of RC structures revolves around the deformation capacity of its primary lateral load resisting system. A more desirable deformation capacity of a structural wall can be achieved by suppressing the premature compression failure modes in its boundary regions. In order to assess the performance of flexurally dominated walls, a simplified approach of experimentally testing RC columns (or prisms) representing wall boundary zones under uniaxial loading is commonly adopted by researchers.

The review of previous experimental studies on rectangular RC prisms representing wall boundary elements suggests that extensive research has been performed on understanding the parameters that induce premature compression failure modes under monotonic compression, pre-strain (tensile strain) prior to reloading monotonically into compression, and cyclic tension-compression loading. However, various loading protocols, adopting a range of tensile-to-compressive (T/C) ratios, have been used in the literature. For instance, Chai and Elayer (1999) and Taleb et al. (2016) have considered a constant (T/C) ratio equal to 5 or 7; Hilson et al. (2014) and Haro et al. (2018) kept the compressive strain constant while the tensile strain increased gradually; whereas Goodsir (1985) and Hilson et al. (2014) adopted a loading protocol with both tensile and compressive strains of increasing order, but with varying (T/C) ratios. Figure 1 shows a sample uniaxial loading protocol with (T/C) ratio = 5. Moreover, these loading protocols adopt arbitrarily decided multiple cycles at a certain strain range. Experimental research on RC bridge columns subjected to symmetric reversed cyclic lateral loading by Nojavan (2015), Acun and Sucuoglu (2010) suggests that large number of cycles at lower drift ratios (up to 3.7%) do not seem to affect the cyclic envelope response of the columns. Studies by Kunnath et al. (1997) and McDaniel et al. (2006) on lightly reinforced bridge columns demonstrate that the load history greatly affects the sequence of failure modes. Goodnight et al. (2013) postulated that the longitudinal bar buckling in circular RC bridge columns is more influenced by the conventional symmetric 3-cycle set loading protocol than the earthquake drift history. Although, these studies evaluate the effect of variation in number of cycles on behaviour of laterally loaded RC bridge columns, they may not directly apply to axially loaded columns representing wall boundary zones.

Therefore, the objective of this research paper is to present a numerical procedure leading to the development of a uniaxial cyclic loading protocol based on various earthquake characteristics, number of inelastic cycles and corresponding strain ranges. The general methodology followed for the loading protocol development, as shown in Figure 2, consists of four steps: (1) selection and scaling of ground motion records; (2) analytical modelling of a typical RC wall; (3) calculation of seismic demands and post-processing of results; and (4) construction of loading protocol. The following sections discuss these steps in detail.

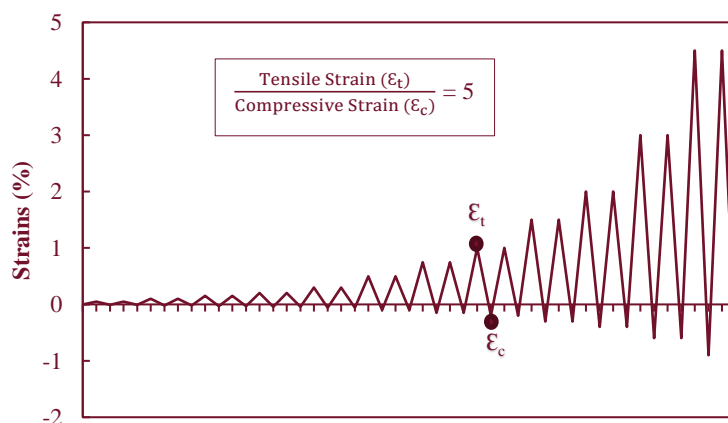


Figure 1: Sample uniaxial cyclic loading protocol with tension-to-compression strain ratio = 5

## 2 METHODOLOGY

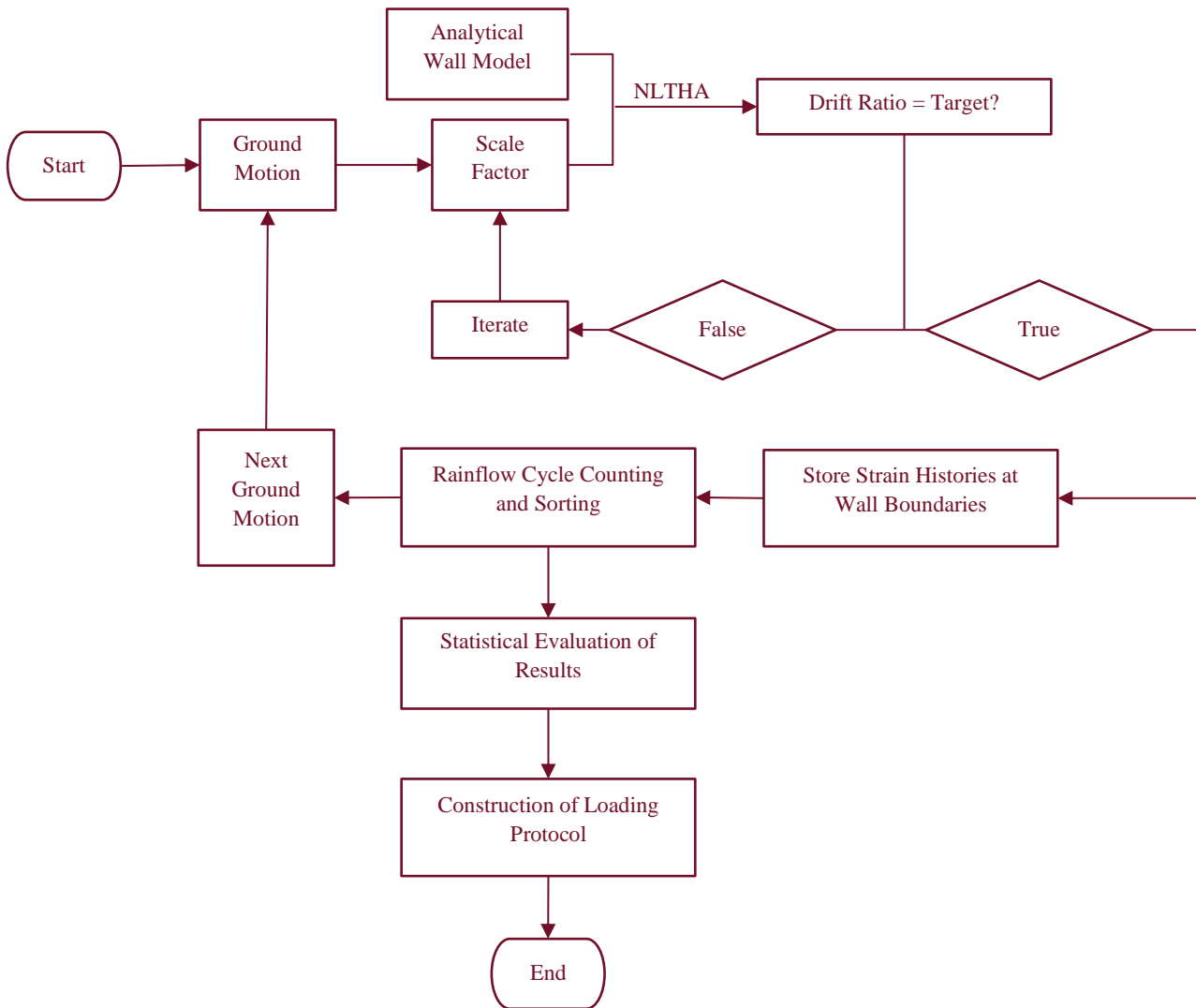


Figure 2: Flow-chart of methodology adopted for loading protocol development

### 2.1 Selection and Scaling of Earthquake Ground Motions

With the aim of developing uniaxial cyclic loading protocol for RC prisms simulating wall boundary zones, a selection of strong ground motions of a particular characteristic is utilized to determine the inelastic strain demands at the wall boundaries. A set of 7 near-field (pulse type) and far-field ground motions, as shown in Table 1, are considered separately to allow for demand comparison. The subduction zone (megathrust type) ground motions are not considered in this study. The ground motions are selected from the PEER ground motion database with the following criteria: moment magnitude greater than 6, recorded on soils categorized by U.S. Geological Survey (USGS) as soil types C and D, and originated from shallow crustal sources (strike-slip or reverse fault mechanisms). The number of ground motions from each earthquake event is limited to one to avoid biased results. Although in one instance, more than one record is selected from the same earthquake event, the earthquake recording stations were at different epicentral distances and have different average shear wave velocities. Out of the two horizontal earthquake ground motion components, the record that generated greater drift demand is utilized. The vertical component of the ground motion is not considered in this research study.

Each ground motion record is scaled such that the maximum response generated by the time-history analysis equals the performance criteria set at the beginning of the analysis. In this study, the maximum drift ratio controls the performance limit state instead of a particular seismic hazard level. For RC walled structures, ACI-374.2R (2013) defines four performance levels in terms of lateral story drift ratios. The scale factor is therefore adjusted to produce the maximum lateral drift ratio around 2-2.5% corresponding to “Near Collapse” limit state.

*Table 1: Ground motion records representative of moderate to high seismicity regions*

Sr. No.	Earthquake Event	Station	Year	Moment Magnitude	Closest Distance to Fault Rupture (km)	Pulse Period $T_p$ (sec)	Average Shear Wave Velocity $V_{s30}$ (m/s)
Near-fault ground motion suite	1	Darfield (New Zealand)	GDLC	2010	7	1.22	344
	2	Chi-Chi (Taiwan)	CHY028	1999	7.62	3.12	542
	3	Christchurch (New Zealand)	Christchurch Botanical Gardens	2011	6.2	5.52	187
	4	Northridge-01	Sylmar – Converter Sta East	1994	6.69	5.19	370.52
	5	Loma Prieta	Gilroy Array #3	1989	6.93	12.82	349.85
	6	Tabas (Iran)	Tabas	1978	7.35	2.05	766.77
	7	Duzce (Turkey)	Duzce	1999	7.14	6.58	281.86
Far-field ground motion suite	1	New Zealand – 02	Matahina dam	1987	6.6	16.1	551.3
	2	Superstition Hills – 02	El Centro Imp. Co. Cent	1987	6.54	18.2	192.05
	3	Loma Prieta	Gilroy Array #7	1989	6.93	22.35	333.85
	4	Loma Prieta	Hollister Differential Array	1989	6.93	24.52	215.54
	5	Landers	Desert Hot Springs	1992	7.28	21.78	359
	6	El Mayor-Cucapah (Mexico)	Michoacan De Ocampo	2010	7.2	13.21	242
	7	Imperial Valley – 06	Delta	1979	6.53	22.03	242.05

Source: PEER NGA-West2 Ground Motion Database

## 2.2 Analytical Wall Model

The loading protocol adopted in laboratories to assess the seismic performance of a structural system should be representative of the cumulative inelastic demands subjected by moderate-to-large magnitude

*Paper 135 – Quasi-static uniaxial cyclic loading protocol for RC columns simulating wall boundary zones*

earthquakes. Therefore, in this study, to obtain realistic strain demands at the wall boundaries, an analytical wall model is utilized that is subjected to earthquake ground motions of various characteristics.

The analytical wall model utilized for the purpose of loading protocol development represents a scaled RC wall with a shear span ratio equal to 3 and subjected to axial load ratio of 5.6%. The wall model is identical to the wall specimen that was recently tested at the Structural Engineering Laboratory of University of Canterbury, thus facilitating calibration of model parameters. Details of the wall specimen and experimental program could be found in Tripathi et al. (2019). The wall is modelled using the Multiple Vertical Line Element Model (MVLEM) developed by Vulcano et al. (1988) and later implemented in OpenSees (McKenna et al. 2000) by Kolozvari et al. (2018). The hysteretic responses of steel and concrete are modelled using the SteelMPF and ConcreteCM models, respectively, available in OpenSees. Figure 3 shows the force-displacement response of the wall model in comparison with the experimental response. While the hysteresis response matches well with the experimental results, the strength degradation observed in the test is not represented by the model. It should be noted that modelling of any specific failure modes relating to slender RC walls is not intended in this study. This is done to get a stable response when the analytical model is subjected to high demands and to avoid any interference due to strength and stiffness deterioration aspects in the load history development. (Krawinkler et al. 2000)

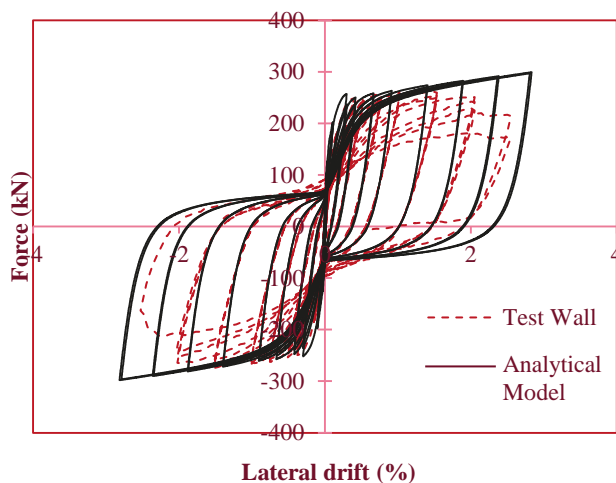


Figure 3: Comparison between experimental and analytical force-displacement hysteresis responses

## 2.3 Calculation of Seismic Demands and Post-processing

### 2.3.1 Time History Analyses

Non-linear time history analyses (NLTHA) are carried out to obtain the wall global and local responses. Each analysis under the effect of a scaled ground motion provides strain histories in the vertical line elements. Out of these, strain histories in the bottom most elements located at wall boundaries are of importance; because these elements are more susceptible to large inelastic strain demands in a flexurally dominated RC wall. Thus, a total of 2 (strain histories per ground motion)  $\times$  7 (ground motions) = 14 strain histories are obtained from each ground motion suite. These strain histories are then utilized in the development of loading protocol, as described in the following sections.

### 2.3.2 Rainflow Cycle Counting

A Matlab<sup>®</sup> script implementing rainflow counting algorithm developed by Irvine (2012) consistent with the procedure described in ASTM-E1049-85 (2005) is employed to count the cycles in the strain histories obtained using the method described above. The rainflow cycle counting algorithm identifies cycles as closed hysteresis loops and provides corresponding ranges (difference between maximum and minimum

peaks). Although the algorithm determines the peak pairs involved in a strain range, the sequence of their occurrences is not preserved. The cycle count and strain ranges thus obtained are arranged in descending order to allow discarding of data below a certain threshold strain range. In this study, threshold strain range is considered equal to yield strain of the reinforcing bars, so that majority of the tensile strains are above the elastic limit.

### 2.3.3 Statistical Evaluation of Response

The cyclic loading protocol development procedures by Krawinkler et al. (2000), Mergos and Beyer (2014), Bazaez and Dusicka (2016) are predominantly convenient for lateral cyclic response assessment of structural components, where the displacement response is assumed to be centred with respect to zero, thereby resulting in a symmetric cycle of equal displacement amplitudes. However in case of wall boundary zones, the strain histories are rather asymmetric, i.e. tensile strain magnitudes are often greater than the corresponding compressive strains.

Thus, development of uniaxial cyclic loading protocol for RC prisms simulating wall boundary regions requires determination of two relationships, between: (1) strain range and cumulative number of cycles, and (2) strain range and tensile or compressive strain. The resultant strain range, corresponding peaks, and cycle count data obtained in the previous step are utilized for this purpose.

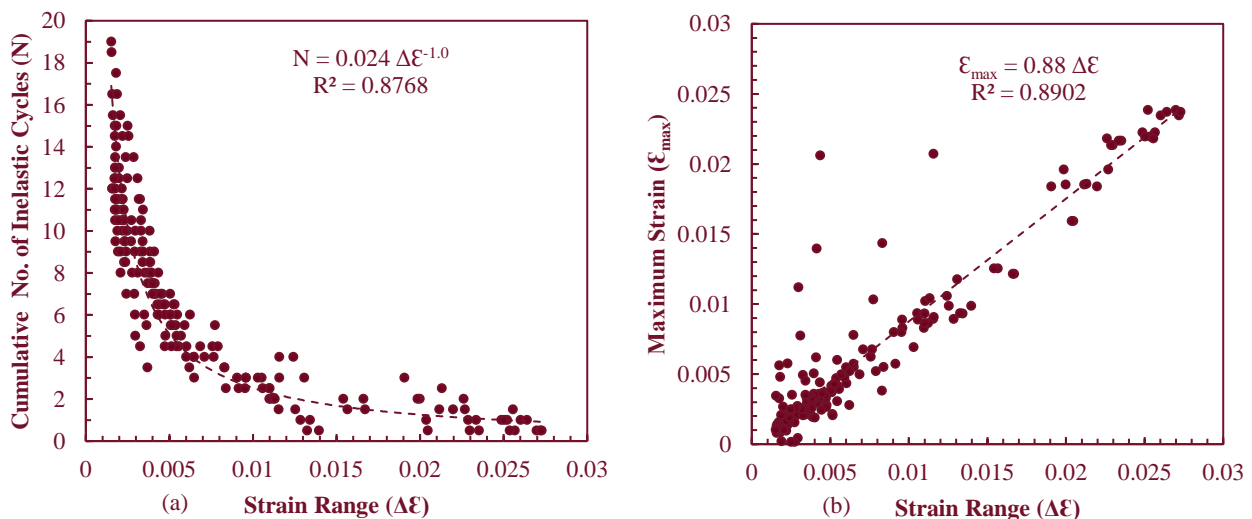


Figure 4: Statistical evaluation of results for sample "near-fault" ground motion suite: (a) relationship between cumulative number of cycles and strain range; (b) relationship between tensile strains and strain ranges

Figure 4 (a) and (b) show the two relationships between the strain range and cumulative number of inelastic cycles, and between the strain range and the tensile strain (or maximum strain), respectively, for the “near-fault” ground motion suite. The first relationship provides the number of cycles beyond a particular strain range ( $\Delta\epsilon$ ) under consideration. For example, say for  $\Delta\epsilon = \epsilon_y = 0.0015$ , there are about 16 cycles outside this strain range. This also signifies that there are around 16 cycles in total within the loading protocol. Similarly, for  $\Delta\epsilon = 0.015$ , there are approximately two cycles ( $N \approx 2$ ) beyond this strain range. The second relationship provides the tensile strain ( $\epsilon_{\max}$ ) associated with the strain range ( $\Delta\epsilon$ ) under consideration. Once, the tensile strain is known, the corresponding compressive strain in a loading cycle can be easily worked out.

## 2.4 Construction of Loading Protocol

The construction of loading protocol follows 3 simple steps: (1) selection of strain ranges in increasing order, (2) calculating the corresponding cumulative number of inelastic cycles ( $N$ ) and number of inelastic cycles ( $n$ ) to reach the strain range under consideration, and (3) calculating the tensile and compressive strains.

Table 2 shows the arithmetic involved in the construction of loading protocol, and Figure 5 illustrates the steps involved in the construction of loading protocol for the same “near-fault” ground motion suite example.

Table 2: Arithmetic involved in construction of loading protocol: Sample results for “near-fault” ground motion suite

Strain Range ( $\Delta\epsilon$ )	Cumulative Inelastic Cycles $N = \frac{0.024}{\Delta\epsilon}$	No. of Inelastic Cycles ( $n$ )	Maximum Strain $\epsilon_{max} = 0.88 * \Delta\epsilon$	Minimum Strain $\epsilon_{min} = \epsilon_{max} - \Delta\epsilon$
0.0015 ( $\epsilon_y$ )	16.0	Round up & Subtract 10.0	0.0013	-0.00018
0.0045 ( $3\epsilon_y$ )	5.3	3.0	0.004	-0.00054
0.009 ( $6\epsilon_y$ )	2.7	2.0	0.008	-0.00108
0.027 ( $18\epsilon_y$ )	0.9	1.0	0.024	-0.00324

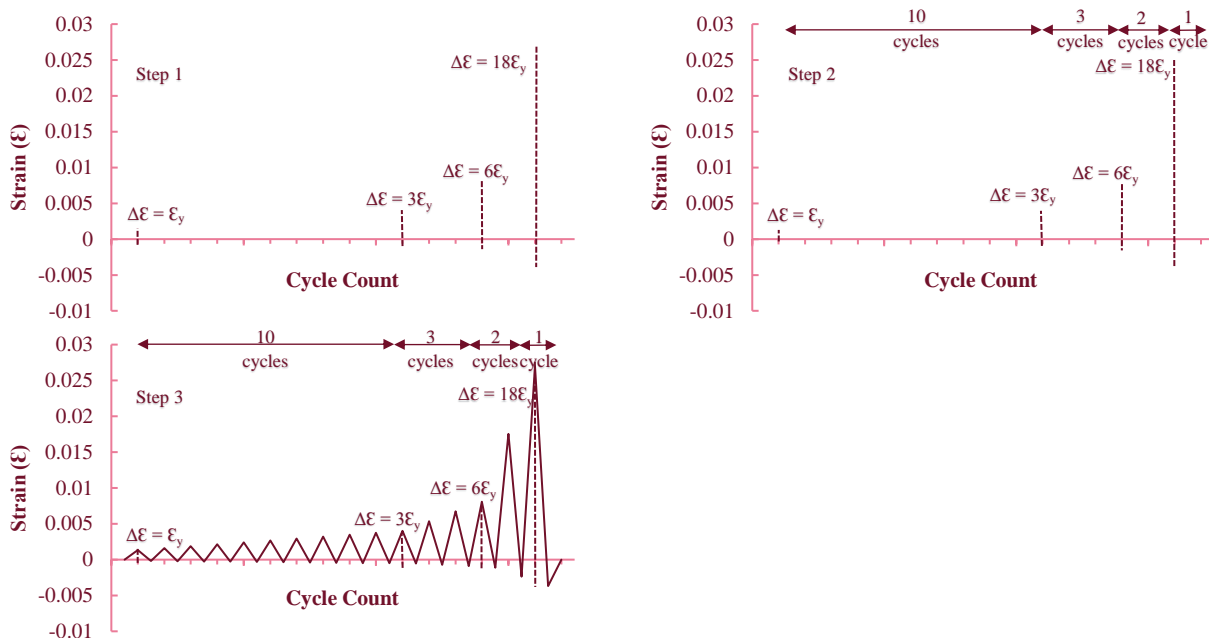


Figure 5: Steps involved in construction of loading protocol: Sample results for “near-fault” ground motion suite

## 3 CONCLUSIONS

Compression failure modes associated with flexurally dominated RC walls are often investigated in laboratories by testing RC columns representing the wall boundary regions under quasi-static uniaxial cyclic

loading. However, there is a lack of consensus among researchers on the choice of number of cycles, and tensile and compressive strain relationship in the adopted loading protocols. This paper presents a numerical procedure leading to the development of a uniaxial cyclic loading protocol representative of moderate-to-large earthquakes of a particular characteristic. The proposed procedure provides realistic distribution of inelastic cycles and corresponding strain ranges in the resulting loading protocol, thus facilitating more rational assessment of the slender RC walls than the current approach of testing under arbitrarily decided tension-compression cycles. Although this study utilizes only near and far-field earthquakes, the proposed methodology could be easily extended to subduction megathrust earthquakes. Nevertheless, further studies are required to evaluate the consistency in results by conducting analyses with different analytical wall models. Also, parametric studies can be performed by comparing loading protocols resulting from earthquakes of various characteristics, different axial load ratios, and various geometrical characteristics of walls.

## 4 REFERENCES

- ACI-374.2R. 2013. *Guide for Testing Reinforced Concrete Structural Elements Under Slowly Applied Simulated Seismic Loads*, American Concrete Institute, Farmington Hills, MI 48331, U.S.A.
- Acun, B. & Sucuoglu, H. 2010. Performance of Reinforced Concrete Columns Designed for Flexure under Severe Displacement Cycles, *Structural Journal*, Vol 107(3).
- ASTM-E1049-85. 2005. *Standard Practices for Cycle Counting in Fatigue Analysis*, ASTM International, West Conshohocken, PA.
- Bazaez, R. & Dusicka, P. 2016. Cyclic Loading for RC Bridge Columns Considering Subduction Megathrust Earthquakes, *Journal of Bridge Engineering*, Vol 21(5), 04016009.
- Chai, Y.H. & Elayer, D.T. 1999. Lateral Stability of Reinforced Concrete Columns under Axial Reversed Cyclic Tension and Compression, *Structural Journal*, Vol 96(5).
- Goodnight, J.C., Kowalsky, M.J. & Nau, J.M. 2013. Effect of Load History on Performance Limit States of Circular Bridge Columns, *Journal of Bridge Engineering*, Vol 18(12) 1383-1396.
- Goodsir, W.J. 1985. *The design of coupled frame-wall structures for seismic actions*, University of Canterbury, <http://hdl.handle.net/10092/7751>.
- Haro, A.G., Kowalsky, M., Chai, Y.H. & Lucier, G.W. 2018. Boundary Elements of Special Reinforced Concrete Walls Tested under Different Loading Paths, *Earthquake Spectra*, Vol 34(3) 1267-1288.
- Hilson, C.W., Segura, C.L. & Wallace, J.W. 2014. Experimental Studies of Longitudinal Reinforcement Buckling in Reinforced Concrete Structural Wall Boundary Elements, *Proc., 10th National Conference in Earthquake Engineering*, Earthquake Engineering Research Institute.
- Irvine, T. 2012. *Rainflow Fatigue Cycle Counting*, <https://vibrationdata.wordpress.com/2012/10/31/rainflow-fatigue-cycle-counting/>.
- Kolozvari, K., Orakcal, K. & Wallace, J.W. 2018. New opensees models for simulating nonlinear flexural and coupled shear-flexural behavior of RC walls and columns, *Computers & Structures*, Vol 196 246-262.
- Krawinkler, H., Parisi, F., Ayoub, A. & Medina, R. 2000. Development of a Testing Protocol for Wood Frame Structures, *CUREE Publ. No. W-02*, Consortium of Universities for Research in Earthquake Engineering, Richmond, California.
- Kunnath, S. K., El-Bahy, A., Taylor, A. & Stone, W. 1997. Cumulative seismic damage of reinforced concrete bridge piers, *Technical Report NCEER-97-0006*, University of Central Florida and National Institute of Standards & Technology.
- McDaniel, C.C., Cofer, W.F., McLean, D.I. & Rodriguez-Marek, A. 2006. Performance of Pre-1975 Concrete Bridges in Cascadia Subduction-Zone Earthquakes, *FHWA Contract DTFH61-03-C-00104, Effects of Long Duration Earthquakes on Bridges*, Washington State Transportation Center (TRAC), Washington State University, Department of Civil & Environmental Engineering.
- McKenna, F., Fenves, G., Filippou, F. & Mazzoni, S. 2000. *Open System for Earthquake Engineering Simulation (OpenSees)* <http://opensees.berkeley.edu/index.php>.
- Mergos, P.E. & Beyer, K. 2014. Loading protocols for European regions of low to moderate seismicity, *Bulletin of*

*Earthquake Engineering*, Vol 12(6) 2507-2530.

- Nojavan, A. 2015. *Performance of Full-Scale Reinforced Concrete Columns Subjected to Extreme Earthquake Loading*, PhD, Civil Engineering, University of Minnesota.
- Taleb, R., Tani, M. & Kono, S. 2016. Performance of Confined Boundary Regions of RC Walls under Cyclic Reversal Loadings, *Journal of Advanced Concrete Technology*, Vol 14(4) 108-124.
- Tripathi, M., Dhakal, R.P. & Dashti, F. 2019. Postyield Behaviour of Ductile RC Walls with Different Boundary Zone Detailing: Experimental Investigation, *Engineering Structures (Under Review)*.
- Vulcano, A., Bertero, V.V. & Colotti, V. Analytical Modeling of RC Structural Walls, *Proc., 9th World Conference on Earthquake Engineering*, 41-46.